

# Modeling multi-longitudinal-mode semiconductor lasers with incoherent feedback

C. Masoller, C. Serrat, and R. Vilaseca

*Departament de Física i Enginyeria Nuclear, Universitat Politècnica de Catalunya, Colom 11, E-08222 Terrassa, Spain*

(Received 26 May 2007; published 11 October 2007)

We study numerically the dynamics of a multi-longitudinal-mode semiconductor laser subject to incoherent optical feedback. The feedback scheme is such that the polarization state of the feedback light is rotated  $90^\circ$ , so that the natural laser mode, TE, is coupled unidirectionally into the orthogonal, unsupported mode, TM. We use traveling-wave equations for the slowly varying complex amplitudes of the two counterpropagating optical fields circulating in the Fabry Pérot cavity, both with TE polarization, coupled to an equation for the carrier population. The carrier equation contains a time-delayed term that takes into account the effect of the incoherent feedback. The model considers a parabolic frequency-dependent gain and does not assume *a priori* a fixed number of active longitudinal modes. We find that moderate feedback levels reduce the total power and increase the number of oscillating longitudinal modes. Larger feedback levels lead to instabilities at both the external cavity frequency  $f_{ext}$  and the relaxation oscillation frequency  $f_{ro}$ . These findings are in good qualitative agreement with experimental observations by Houlihan *et al.* [Opt. Commun. **199**, 175 (2001)]. For even stronger feedback there is square-wave periodic modulation of the total power, with a repetition period close to twice the delay time. In this regime, which consists of a sequence of turn-on and turn-off events driven by the incoherent feedback, the longitudinal modes show in-phase behavior at a frequency close to  $f_{ro}$  accompanied by a slower out-of-phase drift, which is related to variations of the maximum and minimum values of the oscillation amplitude of the modal intensities.

DOI: [10.1103/PhysRevA.76.043814](https://doi.org/10.1103/PhysRevA.76.043814)

PACS number(s): 42.55.Px, 42.60.Mi, 42.65.Sf

## I. INTRODUCTION

Semiconductor lasers are key elements of today's optical communications technology and have immense importance in consumer electronics, being used in CD and DVD players, printers, scanners, etc. Under external perturbations, such as optical feedback, optical injection, and current modulation, these lasers often present instabilities in their optical output. The influence of optical feedback has received specific attention because it can lead either to an improved performance (mode-hopping suppression and linewidth reduction), or to unstable emission (in the form of low-frequency fluctuations and coherence collapse [1]), which has found applications for secure communications.

The effect of polarization-rotated optical feedback has also attracted considerable interest because of its potential for high-frequency pulse generation and all-optical switching. In this scheme the polarization state of the feedback light is rotated  $90^\circ$ , by placing a polarization-rotation device in the external cavity. Hence the mode normally supported by the laser cavity (which we refer to as TE) is coupled into the unsupported orthogonal mode (which we refer to as TM). Two different types of feedback have been studied. In the first type, which we will refer to as polarization-rotated feedback, a quarter-wave plate is inserted in a Fabry-Perot external cavity, with its axes oriented to convert, after two passes through the  $\lambda/4$  plate, TE to TM polarization and vice versa. Alternatively, a half wave plate is placed in a ring external cavity, converting TE to TM light and vice versa after a single pass through the  $\lambda/2$  plate. In both configurations, the TE and TM modes are mutually coupled. In the second type of feedback, which we will refer to as incoherent feedback, an optical isolator is placed in the external cavity to ensure that the TE polarization is completely suppressed of the feed-

back light. Hence the feedback light is TM polarized and does not interfere coherently with the TE field in the laser cavity, acting only as a saturating beam for the carrier density in the active region.

Both polarization-rotated and incoherent feedback can produce fast optical pulses without the need of any high-speed electronics, as already demonstrated in the early 1990s [2–5]. The operating principle behind it is as follows. In the case of polarization-rotated feedback [2–4], if the emission is initially TE polarized, the light reinjected into the cavity is TM polarized, and stimulated emission sustains lasing in this new polarization, but during the next reinjection light is converted back to TE polarization, hence the polarization is self-modulated and there is alternation of TE and TM emission with periodicity  $2\tau$ , where  $\tau$  is the feedback delay time. However, a Fabry-Perot external cavity of high reflectivity gives rise to multiple reflections which ensure that both TM and TE polarizations are simultaneously present in the feedback light. This leads to partially coherent feedback, which was studied experimentally and numerically by Ju and co-workers [6,7], who showed that, with simultaneous coherent and incoherent feedback, the unsupported TM polarization does not lase.

In the case of incoherent feedback, the feedback can modulate the carrier density inducing self-sustained relaxation oscillations, with a repetition rate governed by the relaxation oscillation frequency. This effect was predicted by Otsuka and Chern [5] and observed recently in [6,8]. However, incoherent feedback can also lead to pulses with a periodicity controlled by the feedback delay time, which were observed by Yen *et al.* [9]: when the feedback is sufficiently strong, it depletes almost completely the carrier population and thus the laser turns off, but once the laser is off the feedback ceases to act, and thus the laser turns on again. Thereby, strong enough incoherent feedback causes the laser

to switch between on and off states with periodicity approximately  $2\tau$ . Recently, Gavrielides *et al.* [10] demonstrated experimentally that incoherent feedback can also generate polarization self-modulation, with the TE and TM polarizations exhibiting square-wave antiphase oscillations whose frequency is governed by the external cavity frequency. Based on a model that considers both TE and TM polarizations [11], Gavrielides *et al.* showed that these oscillations appear for a broad range of parameters, provided that the feedback level is strong and the differential losses in the normally unsupported TM mode are small.

Recently, novel applications of incoherent feedback have been proposed. Oria and co-workers [12,13] placed a frequency-sensitive filter (Cs vapor cell) in the way of the feedback beam to spectrally modulate the feedback intensity and observed two different emission frequencies with nearly the same output power. This frequency bistability can have potential applications for all-optical logic gates. A model was proposed in [14] that, by taking into account thermal and gain saturation effects, explained the linear variation of the laser frequency with the feedback strength that was observed in [12,13], and that originated the frequency bistability. The model allowed time-dependent solutions to be studied, and in particular, the hysteresis cycle produced by sweeping back and forth the laser emission frequency across the resonance of the filter.

The incoherent feedback scheme was recently proposed theoretically as a novel approach for inducing passive mode locking without using any saturable absorber, but exploiting the polarization of the light [15]. In this approach mode locking is achieved by the delayed reinjection of the polarization-rotated laser output. The laser operates in a multimode regime due to coherent optical feedback from an external cavity with delay time  $\tau_1$ , and a fraction of the laser output passes through a polarization-rotation device before being reinjected into the laser, after a delay time  $\tau_2$ . In regions of the parameter space  $(\tau_1, \tau_2)$  mode-locking occurs: the optical spectrum of the orthogonal polarizations shows a frequency comb with peaks separated by  $1/\tau_1$ , and the two polarizations exhibit similar time traces, one wave form being a scaled replica of the other, with a temporal shift between them given by  $\tau_2 - \tau_1$ . The method was proposed for vertical-cavity surface-emitting lasers and optical amplifiers, but is expected to be suitable also for edge-emitting lasers.

The synchronization of semiconductor lasers with orthogonal feedback and/or orthogonal injection has also been investigated [16–21] and it has been reported that incoherent and polarization-rotated feedback schemes have the advantage over coherent optical feedback that the laser synchronization does not require a careful matching of the laser frequencies.

In spite of all the attention that incoherent feedback has attracted, few studies have addressed the issue of multi-longitudinal-mode emission. To the best of our knowledge, multimode emission was studied only in Refs. [8,9,22,23]. Huyet and co-workers [22] observed experimentally that incoherent feedback enhanced instabilities at low frequencies (associated with an enhancement of the mode partition noise) and at high frequencies (related to the relaxation oscillation frequency and the external cavity frequency). Cheng *et al.*

[23] showed experimentally that under appropriate conditions, incoherent feedback can significantly reduce, and even completely suppress, longitudinal mode hopping. In a more recent study Cheng and Yen [8] characterized experimentally and numerically the multimode behavior as a function of the external cavity frequency and found a structure of bands: the laser oscillated in different longitudinal modes in two regions of the external cavity frequency, separated by a region where longitudinal mode hopping occurred. In addition, Yen *et al.* [9] observed in that, under strong feedback conditions, the switching between on and off states was accompanied by an enhancement of multimode emission.

The objective of the present work is to study the influence of incoherent feedback on the multimode dynamics of semiconductor lasers. We use a model consisting of two equations for the counterpropagating fields, both with TE polarization, coupled to an equation for the carrier population. This model, which takes into account a parabolic frequency-dependent gain and does not assume *a priori* a fixed number of active modes, has been employed to study multimode behavior in the presence of coherent optical feedback [24–26] and optical injection [27]. Two of us recently studied the intrinsic multimode dynamics (without any external perturbation) and found deterministic out-of-phase modal oscillations which leave the sum of total modal intensities nearly constant [28].

Here we extend the model to account for incoherent feedback, assuming that the reinjected light does not interfere coherently with the lasing field but depletes the shared carrier reservoir [5,6,29]. The feedback is included through a time-delayed term in the carrier equation, which acts as a saturating intensity. As is shown below, depending on the strength of this delayed feedback term, different dynamic regimes are found. For moderate feedback there are oscillations of the output power whose repetition rate is mainly determined by relaxation oscillations; for stronger feedback, there are square-wave oscillations of the output power whose repetition rate is governed by the external cavity delay time. By using spectral filtering techniques we investigate the underlying dynamics of the individual longitudinal modes. We find that the modal intensities present in-phase oscillations in the fast time scale of relaxation oscillations, accompanied by a slow out-of-phase modulation, related to a drift of the maximum and minimum values of the oscillation amplitude of the modal intensities. These results are in good qualitative agreement with the experimental observations of Ref. [22]; however, we also find some differences. Specifically, in our model the total intensity is either constant or presents oscillations in the GHz frequency range (related to the relaxation oscillation frequency and the external cavity frequency), while in [22], a regime of slow oscillations of triangular shape was observed, with a frequency in the MHz range.

This paper is organized as follows. Section II presents the model, Sec. III presents the numerical results, and Sec. IV presents a summary and a discussion of the model predictions and the experimental observations.

## II. MODEL

The model studied in [28] is extended to account for incoherent optical feedback, where the output of the laser is

rotated  $90^\circ$  and reinjected into the laser after a round-trip delay time  $\tau$ .

The optical field in the laser cavity is written as

$$\tilde{E}(z,t) = E(z,t)e^{-i\omega_0 t} + \text{c.c.}, \quad (1)$$

where  $E(z,t) = E^+(z,t)e^{ik_0 z} + E^-(z,t)e^{-ik_0 z}$ , with  $E^+(z,t)$  and  $E^-(z,t)$  being the complex amplitudes of the fields circulating forward and backward in the Fabry-Perot laser cavity, with TE polarization.  $\omega_0$  is the reference frequency and  $k_0$  is the corresponding propagation constant,  $k_0 = \eta\omega_0/c$ , with  $\eta$  being the background refractive index, and  $c$  the velocity of light in vacuum. The spatial grating in the longitudinal  $z$  direction in the carrier density profile, due to the standing wave, can be written as a Fourier expansion with a spacing of half a wavelength:

$$\mathcal{N}(z,t) = N(z,t) \left[ 1 + \sum_p N_p(t) (e^{2ipk_0 z} + e^{-2ipk_0 z}) \right], \quad (2)$$

where  $N(z,t)$  is the envelope of the carrier grating.

As was discussed in [28], an important simplification of the model is that the contribution of terms proportional to  $e^{\pm 2ipk_0 z}$  for any  $p \neq 0$ , to the dynamical evolution of the slowly varying quantities  $E^\pm(z,t)$  and  $N(z,t)$  can be neglected. The terms proportional to  $e^{\pm 2ipk_0 z}$  represent the ‘‘fast’’ carrier grating that arises due to holes burned by the counterpropagating optical fields, and has a characteristic length of half a wavelength (typically, less than  $0.75 \mu\text{m}$ ). The ‘‘slow’’ grating, represented by  $N(z,t)$ , arises due to the interaction of the different longitudinal modes, and can have a much longer characteristic length [30]. Typical values of the carrier lifetime and the carrier diffusion rate in semiconductor media are of the order of  $0.5\text{--}2 \text{ ns}$  and  $0.3\text{--}3.0 \mu\text{m}^2/\text{ns}$ , respectively, giving a diffusion length of the order of  $0.4\text{--}2.4 \mu\text{m}$ . This suggests that carrier diffusion can be fast enough to wash out most of the fast grating, but not fast enough to wash out the slow grating, which can have a significant impact on the longitudinal modes dynamics [30].

With this simplification the equations for the slowly varying variables  $E^\pm(z,t)$  and  $N(z,t)$  are

$$\frac{\eta}{c} \frac{\partial E^\pm}{\partial t} \pm \frac{\partial E^\pm}{\partial z} = \frac{a_{te}}{2} \left[ -i\alpha N + (N - N_0) \left( 1 + G_d L^2 \frac{\partial^2}{\partial z^2} \right) \right] E^\pm - \alpha_i E^\pm + F_{E^\pm}, \quad (3)$$

$$\frac{\partial N}{\partial t} = J - \gamma_{\parallel} N - a_{te} (N - N_0) (|E^+|^2 + |E^-|^2 + P_m). \quad (4)$$

Here  $N_0$  is the transparency carrier density,  $a_{te}$  is the linear gain coefficient,  $\alpha$  is the linewidth enhancement factor, and  $\alpha_i$  represents the internal losses. The term proportional to  $G_d$  represents the parabolic frequency-dependent gain,  $G_d = c^2 / (2\pi L \eta \Delta \nu_g)^2$ , with  $L$  being the laser cavity length and  $\Delta \nu_g$  the gain bandwidth (typically of the order of THz). The noise sources  $F_{E^\pm}(t, z)$  are considered as Gaussian with zero mean, satisfying

$$\langle F_{E^\pm}(z,t) F_{E^\pm}^*(z,t') \rangle = \frac{\eta \gamma_{\parallel}}{c} \beta N(z,t) \delta(t-t'), \quad (5)$$

where  $\beta$  is the spontaneous emission factor [31].

In the carrier equation (4),  $J$  is the pump parameter,  $\gamma_{\parallel}$  is the carrier decay rate, and the last term takes into account phenomenologically the polarization-rotated reinjected light, which does not interfere with the lasing TE field but depletes the shared carrier reservoir. The reinjected beam is proportional to the outgoing beam at the right end of the laser (the laser output is detected at the left end,  $z=0$ ),

$$P_m(z,t) = \gamma |E^+[L, t - \tau - \eta(L-z)/c]|^2, \quad (6)$$

where  $\gamma$  is a dimensionless parameter that characterizes the strength of the feedback ( $0 < \gamma < 1$  since the reinjected power is necessarily lower than the emitted power),  $\tau = 2L_{ext}/c$  is the round-trip delay time in the external cavity, and  $\eta(L-z)/c$  takes into account the extra delay due to propagation inside the laser. It is worthwhile to note that in Eq. (4) the gain coefficient  $a_{te}$  is, in a first step, assumed to be the same for both TE and TM polarizations.

Equations (3) and (4) are supplemented with the usual boundary conditions:

$$E^+(0,t) = \sqrt{R_1} E^-(0,t), \quad (7)$$

$$E^-(L,t) = \sqrt{R_2} E^+(L,t), \quad (8)$$

where  $R_1$  and  $R_2$  are the reflectivities of the laser facets.

The model has approximated steady-state monochromatic solutions that are associated with the longitudinal modes of the active cavity [28]. These solutions are

$$E^\pm(z,t) = \mathcal{E}_m^\pm \exp[\pm i(k_m - k_0)z - (\omega_m - \omega_0)t], \quad (9)$$

$$N(z,t) = \mathcal{N}_m, \quad (10)$$

where  $m$  indicates a particular longitudinal mode. Assuming that the reference frequency  $\omega_0$  is the frequency of the longitudinal mode closest to the gain peak, which we will refer to as the  $n$ th mode, i.e.,  $k_0 = n\pi/L = \eta\omega_0/c$ , for the  $m$ th mode we have

$$k_m = k_0 + (m-n)\pi/L + ik_i = k_r + ik_i. \quad (11)$$

Here,  $k_r$  and  $k_i$  are the real and imaginary parts of the wave vector,  $k_r = k_0 + (m-n)\pi/L$ , and  $k_i$  is given by the boundary conditions

$$\mathcal{E}_m^+ = \mathcal{E}_m^- \sqrt{R_1}, \quad (12)$$

$$e^{2k_i L} = \sqrt{R_1 R_2}. \quad (13)$$

Substituting Eqs. (9) and (10) in Eqs. (3) and (4) gives

$$(1 + \gamma) |\mathcal{E}_m^+|^2 + |\mathcal{E}_m^-|^2 = \frac{J - \gamma_{\parallel} \mathcal{N}_m}{a_{te} (\mathcal{N}_m - N_0)}, \quad (14)$$

$$a_{te} (\mathcal{N}_m - N_0) / 2 = \alpha_i - k_i L, \quad (15)$$

$$\frac{\eta(\omega_m - \omega_0)}{c} = \frac{a_{te}\alpha\mathcal{N}_m}{2} + \frac{(m-n)\pi}{L}, \quad (16)$$

where we have neglected, in the carrier equation, the imaginary part of the wave vector, and in the field equation, terms proportional to  $G_d L^2 k_r^2$ ,  $G_d L^2 k_i^2$ , and  $G_d L^2 k_r k_i$ , that are  $\ll 1$  [28].

Equation (15) implies that the steady-state value of the carrier density,  $\mathcal{N}_m$ , is not modified by the feedback. Thus the solitary laser intensity (for  $\gamma=0$ ) is

$$|\mathcal{E}_{m,sol}^+|^2 = \frac{J - \gamma_{\parallel}\mathcal{N}_m}{a_{te}(\mathcal{N}_m - N_0)(1 + 1/R_1)}. \quad (17)$$

Comparing Eqs. (14) and (17) it is observed that the feedback leads to a decreased intensity as

$$|\mathcal{E}_m^+|^2 = \frac{1 + 1/R_1}{1 + 1/R_1 + \gamma} |\mathcal{E}_{m,sol}^+|^2. \quad (18)$$

It is also worth noting that the feedback does not modify the lasing threshold, which is  $J_{th} = \gamma_{\parallel}\mathcal{N}_m$ .

Equation (18) indicates that the maximum output power reduction occurs when all the emitted light is reinjected into the laser and  $\gamma=1$ . In the limit  $R_1=1$ , the laser output is reduced to about 2/3 of the solitary laser output. However, Houlihan *et al.* [22] observed experimentally a reduction of the slope efficiency of about 50% when reinjecting about 70% of the light, without threshold change. This observation can be explained by different gain coefficients for the TE and TM polarizations,  $a_{te}$  and  $a_{tm}$ , respectively. Thus redefining the feedback parameter as  $\gamma = \gamma a_{tm}/a_{te}$ , if  $a_{tm} > a_{te}$  then  $\gamma$  can be larger than 1; hence the output power can be below 2/3 of the solitary laser power, even when reinjecting less than 100% of the output.

The time evolution of the individual longitudinal modes can be studied by applying a standard filtering technique in the frequency domain. The amplitude of the  $m$ th longitudinal mode at the laser output near the  $z=0$  face,  $E_m(t)$  [which is assumed can vary in time much more slowly than the mode beat frequency  $\nu_b = c/(2\eta L)$ ], can be calculated by first Fourier transforming in frequency space the quantity  $\sqrt{1-R_1}E^-(0,t)$  and then performing a convolution with a filter centered at the modal frequency  $\omega_m$ , given by Eq. (16). Inverse transforming gives the time-dependent modal intensity,  $I_m(t) = |E_m(t)|^2$ . The *incoherent* intensity, defined as the sum of the modal intensities

$$I_i(t) = \sum_m |E_m(t)|^2 \quad (19)$$

and the *coherent* intensity

$$I_c(t) = (1 - R_1)|E^-(0,t)|^2 = \left| \sum_m E_m(t) \right|^2, \quad (20)$$

differ by terms that oscillate at multiples of the beat frequency  $\nu_b$  and are too fast to be detected in the experiments (typically,  $\nu_b > 100$  GHz). Thus in the following section we present results concerning the dynamics of the individual modal intensities and that of their incoherent sum.

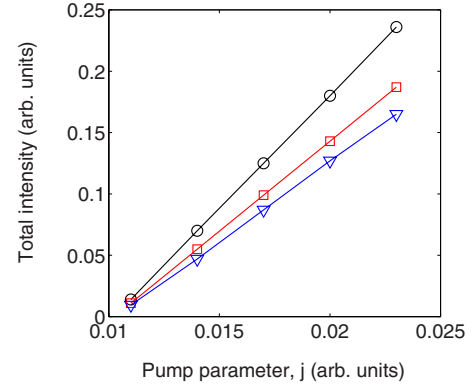


FIG. 1. (Color online) LI curve. The feedback levels are 0 (circles), 0.5 (squares), and 1.0 (triangles).

### III. RESULTS

The model equations were integrated, with the variables  $z$  and  $t$  re-scaled to  $L$  and  $\eta L/c$ , respectively, using integration steps  $\Delta z = \Delta t = 1/300$ . The initial conditions are with the optical fields at the noise level and the carrier density at approximately the transparency value. The parameters used are the same as in [28]:  $L = 275 \mu\text{m}$ ,  $a_{te}N_0L/2 = 0.088$ ,  $2\alpha_i/(a_{te}N_0) = 0.79$ ,  $\gamma_{\parallel}(L\eta/c) = 0.0049$ ,  $\alpha = 4$ ,  $G_d = 5 \times 10^{-5}$ ,  $R_1 = R_2 = 0.95$ , and  $\beta = 10^{-6}$ . The delay time is  $\tau = 5$  ns. The injection current parameter  $j = JL\eta/c$  and the feedback coefficient  $\gamma$  are varied to study different dynamical regimes.

Figure 1 displays the total incoherent intensity vs the injected current ( $L$ - $I$  curve) for the solitary laser (circles) and for two feedback levels. We plot the mean temporal value of the intensity, because multimode emission and/or feedback lead to non-cw operation, as shown below. It can be observed that the incoherent feedback decreases the intensity without modifying the threshold, in good agreement with the analysis of the previous section.

The underlying multimode emission, for a pump parameter slightly above threshold, is presented in Figs. 2 and 3. Figure 2 displays the time evolution of the modal intensities and their incoherent sum, for the solitary laser and for two increasing feedback levels. The modal intensities and the incoherent sum were filtered with a 500 MHz bandwidth filter to simulate the experimental detection bandwidth (similar results were found for other filter bandwidths). Figure 3 displays the optical power spectrum, left column, and the intensity power spectrum, right column, of the total incoherent sum (top trace, shifted vertically for clarity), of the dominant longitudinal mode (middle trace, red online) and of one side mode (lower trace, blue online).

It is observed that without feedback, Fig. 2(a), the laser emits almost in a single longitudinal mode, the intensities of the other modes being at the noise level. The optical power spectrum, Fig. 3(a), reveals a dominant peak at frequency  $\omega_{-1}$  ( $\omega_0$  is the mode closest to the gain peak), with a large side-mode suppression ratio. The intensity power spectrum of the incoherent intensity [Fig. 3(b) top line], presents a peak at the relaxation oscillation frequency,  $f_{ro} \sim 1.25$  GHz. This peak is observed because the 500 MHz filter used is a smooth filter that does not have a sharp cutoff, and thus it

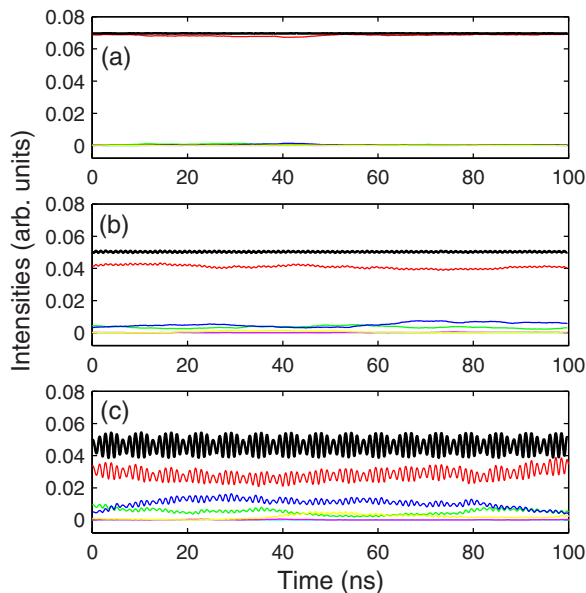


FIG. 2. (Color online) Time evolution of the modal intensities (gray lines, color online) and of the total intensity (black line) for  $j=0.014$  and  $\gamma=0$  (a),  $0.75$  (b),  $1.0$  (c).

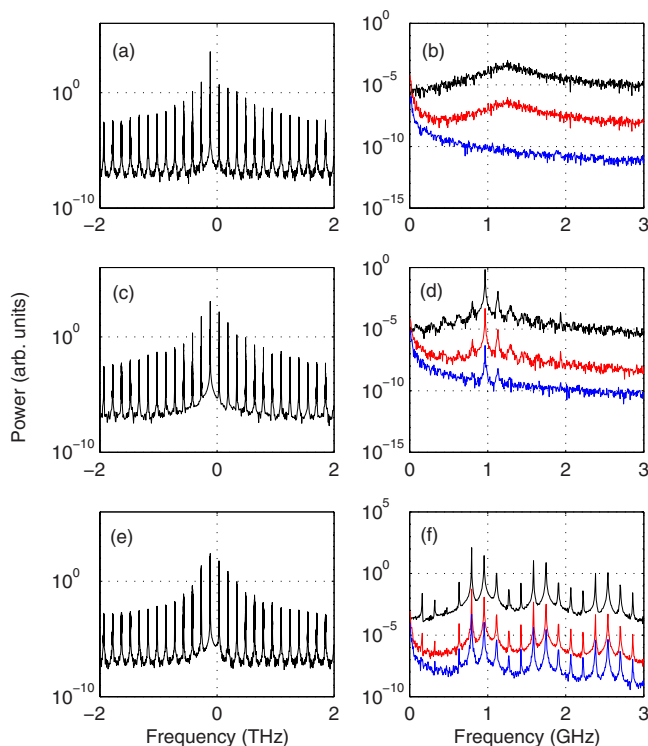


FIG. 3. (Color online) Left: optical power spectrum; right: intensity power spectrum of the total intensity (top curve, black online), of the main longitudinal mode  $i=-1$  (middle curve, red online), and of the neighboring mode  $i=0$  (bottom, blue online). The spectra are shifted vertically for clarity: the top curve by  $10^3$ , the bottom curve by  $10^{-1}$ . Parameters are as in Fig. 2:  $j=0.014$  and  $\gamma=0$  (a),(b);  $0.75$  (c),(d);  $1.0$  (e),(f).

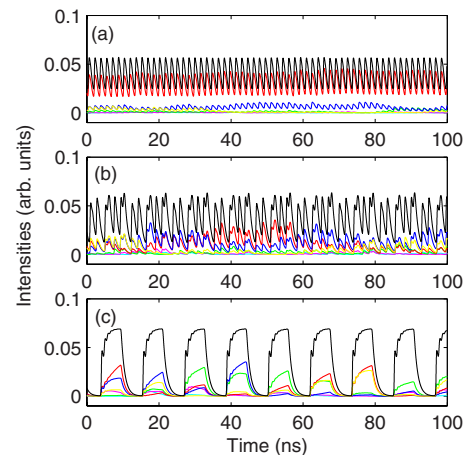


FIG. 4. (Color online) Time evolution of the modal intensities (gray lines, color online) and of the total intensity (black line) for  $j=0.014$  and  $\gamma=1.5$  (a),  $1.75$  (b), and (c)  $2.0$ .

reduces but does not completely eliminate frequencies above  $500$  MHz.

In the intensity power spectrum of the dominant and side modes [Fig. 3(b) middle and bottom lines], the noise at low frequencies is much larger than that in the total intensity. This enhancement, referred to as *mode partition noise*, is a consequence of anticorrelated fluctuations of the individual longitudinal modes due to carrier competition [32], and is known to occur also in vertical-cavity surface-emitting lasers (VCSELs), in transverse-mode competition [33], and in the competition of two orthogonal linear polarizations [34].

Moderate feedback levels reduce the power of the dominant mode and increase the power of other modes, as shown in Figs. 2(b) and 2(c). The spectral broadening can be observed in the optical power spectrum, Figs. 3(c) and 3(e). In the intensity power spectrum, Figs. 3(d) and 3(f), the main peak is enhanced and its frequency decreases [the peak is at  $f_{max} \sim 1$  GHz in Fig. 3(d) and at  $\sim 0.8$  GHz in Fig. 3(f)]. Additional peaks appear at frequencies  $f_{max} \pm f_{ext}$ , where  $f_{ext} \sim 0.16$  GHz is the external cavity frequency, which is slightly lower than  $1/\tau$ . In Fig. 3(f) we observe that there is frequency locking, since the main peak is an integer multiple of  $f_{ext}$  ( $f_{max}/f_{ext}=5$ ). The corresponding time evolution of the total intensity, Fig. 2(c), is quasiperiodic.

Figures 4 and 5 display the temporal evolution and the spectra for larger feedback levels. Periodic, Fig. 4(a), quasiperiodic, Fig. 4(b), and square-wave, Fig. 4(c), oscillations of the total intensity are observed. The square-wave modulation has a periodicity of about  $11.5$  ns, which is slightly larger than  $2\tau$ , and is due to a repetition of turn-on and turn-off events. The incoherent feedback is strong enough to turn off the laser; however, once the laser turns off, after a round trip in the external cavity (i.e., after about  $5$  ns) there is no orthogonal reinjected light and, since the pump current is above the threshold, the laser switches on again, only to turn off after another round trip in the external cavity, i.e., when the reflected orthogonal light re-enters the cavity and depletes, again, the carrier density.

The optical power spectra, displayed in the left column of Fig. 5, show that, as the feedback increases, the number of

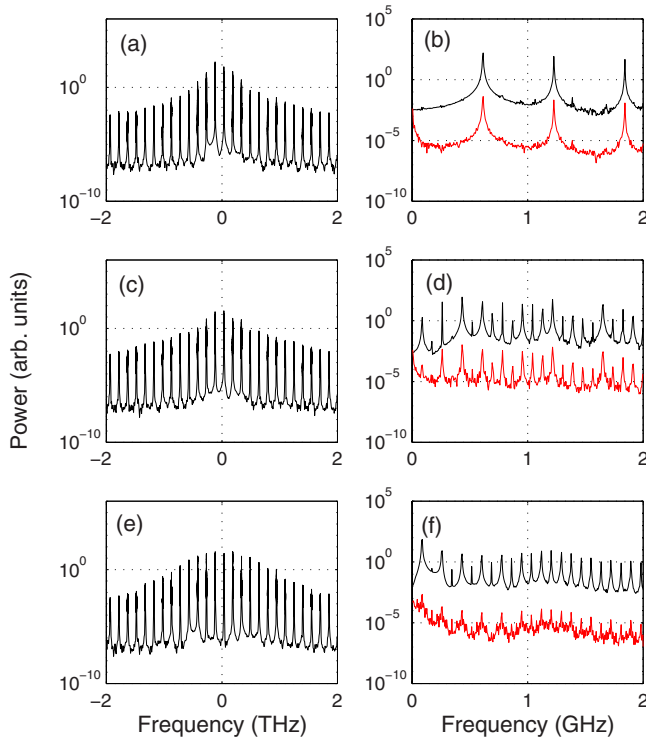


FIG. 5. (Color online) Left: optical power spectrum; right: intensity power spectrum of the total intensity (top, shifted vertically for clarity by  $10^3$ ) and of the main longitudinal mode (bottom). Parameters are as in Fig. 4:  $j=0.014$  and  $\gamma=1.5$  (a), (b); 1.75 (c), (d); 2.0 (e), (f).

active longitudinal modes continues to increase, and the intensity power spectra, displayed on the right column of Fig. 5, show that the frequency of the dominant peak continues to decrease.

The spectra corresponding to the periodic oscillations displayed in Fig. 4(a) is shown in Fig. 5(b), and consists of a main peak at  $f_{max} \sim 0.61$  GHz and its harmonics. The frequency of the main peak is in a locking region with  $f_{ext}$  ( $f_{max}/f_{ext} \sim 4$ ).

For larger feedback the locking is broken and in the intensity power spectra, Fig. 5(d), we observe again two competing frequencies: there is a low frequency peak whose frequency (0.087 GHz) has moved towards a value close to  $f_{ext}/2$  and thus reflects the modulation with period  $2\tau$  describe above, and the main peak at 0.435 GHz. The corresponding time evolution of the total intensity, Fig. 4(b), is quasiperiodic. Finally, for even stronger feedback, the intensity power spectrum, Fig. 5(f), of the square-wave modulation displayed in Fig. 4(c), shows that the low frequency peak at  $f_{ext}/2$  clearly dominates the spectrum.

The oscillations of the longitudinal modes displayed in Fig. 4 are mainly in phase; however, when they are plotted in a longer time scale, displayed in Fig. 6, a slow out-of-phase modal drift is observed: the modes alternate in having the largest power, and there are temporal variations of the maximum and minimum values of the intensities of the individual modes.

Figures 7 and 8 display the temporal evolution and the

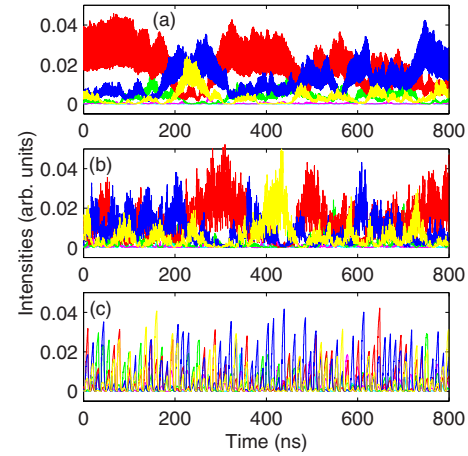


FIG. 6. (Color online) Time evolution of the modal intensities in a longer time scale, for the same parameters as in Fig. 4 (the total intensity is not shown for clarity).

spectra for a larger pump parameter, about twice the threshold. We observe that the effect of the feedback is again an increase of the number of active longitudinal modes and a reduction of the total power. In the absence of feedback the dynamics is almost single mode [Fig. 7(a)]. Moderate feedback levels induce large oscillations in several longitudinal modes, which are out of phase such that the total intensity is nearly constant [Fig. 7(b)]. Larger feedback levels lead to fast oscillations of the total and modal intensities [Figs.

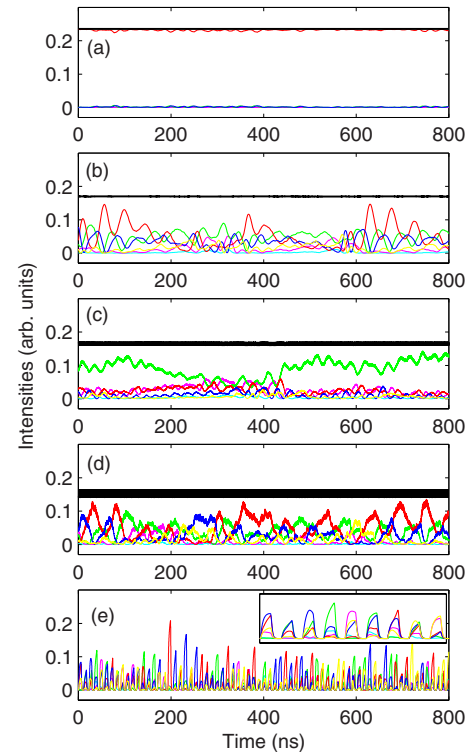


FIG. 7. (Color online) Time evolution of the modal intensities and of the total intensity for  $j=0.023$  and  $\gamma=0$  (a), 0.75 (b), 1.0 (c), 1.5 (d), and 2.0 (e). In (e) the total intensity is not shown for clarity and the inset displays a detail of the time evolution.

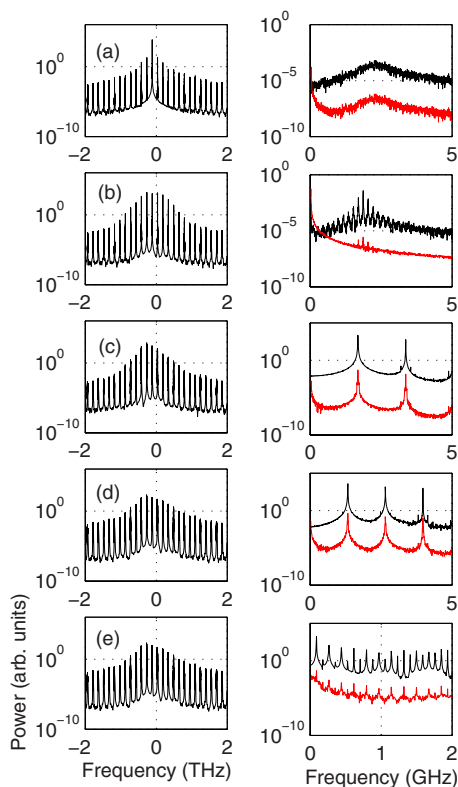


FIG. 8. (Color online) Left column: optical power spectrum. Right column: intensity power spectrum of one longitudinal mode and of the total intensity (shifted vertically for clarity by  $10^3$ ). The pump parameter is  $j=0.023$  and the feedback levels are as in Fig. 6,  $\gamma=0$  (a), 0.75 (b), 1.0 (c), 1.5 (d), and 2.0 (e).

7(c)–7(e)], which are accompanied by slower alternation of the dominant mode. In the intensity power spectrum we observe a frequency locking regime where the external cavity frequency is almost not present in the spectra at low frequencies [similar to that shown in Fig. 5(b)]. For strong enough feedback we again observe square-wave modulation of the total intensity [displayed in the inset of Fig. 7(e)] with a repetition period slightly larger than twice the external cavity delay time. It is noticed that many longitudinal modes turn on simultaneously and this in-phase behavior is accompanied by a slower drift of their relative amplitudes. In the intensity power spectrum, Fig. 8(e), it is observed that the peak at  $f_{ext}/2$  dominates, as it occurred for lower  $j$ , in Fig. 5(f).

#### IV. DISCUSSION AND CONCLUSIONS

We studied the dynamics of a multi-longitudinal-mode semiconductor laser subject to incoherent optical feedback, based on traveling-wave equations that take into account a

parabolic frequency-dependent gain profile and phase-amplitude coupling. The feedback was taken into account through a delayed term in the carrier equation, that acts as a saturating intensity for the carriers in the active region, but it does not interfere coherently with the lasing field. For moderate feedback we found oscillations of the total intensity which correspond to relaxation oscillations modulated by the external cavity delay time; for stronger feedback, the total intensity shows square-wave oscillations with a periodicity governed by the delay time. In both cases, the longitudinal modes present fast in-phase oscillations, accompanied by a slow out-of-phase modulation, related to a drift of the extreme values of the modal oscillations. While periodic and quasiperiodic oscillations were observed in a wide range of parameters, in good agreement with the observations of [6,8], square-wave modulation was only found for values of the feedback parameter  $\gamma > 1$ , related to a larger gain coefficient for TM light than for TE light. This can be due to, e.g., different self- and cross-gain saturation, among other factors, as pointed out in Sec. II and in Ref. [22].

While our model provides a qualitative explanation for several features observed experimentally by Houlihan *et al.* [22], such as the large output power reduction and the onset of instabilities at the relaxation oscillation frequency and the external cavity frequency, it is interesting to also notice some differences. Specifically, for weak feedback levels it was observed in [22] that the total laser intensity presents a time trace with slow oscillations of triangular shape, of frequency of the order of 1 MHz, and that the individual modes were pulsing regularly with the same repetition frequency as the triangular signal. In our model, the total intensity is either nearly constant, due to anticorrelated oscillations of the individual modes, or presents fast oscillations, due to their in-phase behavior, with a frequency governed by the relaxation oscillation frequency and the external cavity frequency.

We speculate that models taking into account four-wave mixing [35] and spatial hole burning effects through nonlinear gain coefficients [36,37] or an expansion in moments of the carrier density [38], can perhaps give a more accurate description, but the inclusion of incoherent feedback in these models is not trivial, and we consider that our model takes into account the main factors characterizing incoherent feedback.

#### ACKNOWLEDGMENTS

The work was supported in part by Spanish Ministerio de Educación y Ciencia through project FIS2005-07931-C03-03 and the "Ramón y Cajal" Program. C.M. also acknowledges support of U.S. Air Force Office of Scientific Research under Grant No. FA9550-07-1-0238.

- [1] J. Ohtsubo, *Progress in Optics*, edited by E. Wolf (North-Holland, Amsterdam, 2002), Vol. 44, Chap. 1.
- [2] W. H. Loh, A. T. Schremer, and C. L. Tang, *IEEE Photonics Technol. Lett.* **2**, 467 (1990).
- [3] W. H. Loh, Y. Ozeki, and C. L. Tang, *Appl. Phys. Lett.* **56**, 2613 (1990).
- [4] W. H. Low and C. L. Tang, *IEEE J. Quantum Electron.* **27**, 389 (1991).
- [5] K. Otsuka and J. L. Chern, *Opt. Lett.* **16**, 1759 (1991).
- [6] R. Ju and P. S. Spencer, *J. Lightwave Technol.* **23**, 2513 (2005).
- [7] R. Ju, Y. Hong, and P. S. Spencer, *IEE Proc.: Optoelectron.* **153**, 131 (2006).
- [8] D. L. Cheng and T. C. Yen, *Opt. Commun.* **271**, 503 (2007).
- [9] T. C. Yen, J. W. Chang, J. M. Lin, and R. J. Chen, *Opt. Commun.* **150**, 158 (1998).
- [10] A. Gavrielides, T. Erneux, D. W. Sukow, G. Burner, T. McLachlan, J. Miller, and J. Amonette, *Opt. Lett.* **31**, 2006 (2006).
- [11] T. Heil, A. Uchida, P. Davis, and T. Aida, *Phys. Rev. A* **68**, 033811 (2003).
- [12] A. F. A. da Rocha, P. C. S. Segundo, M. Chevrollier, and M. Oria, *Appl. Phys. Lett.* **84**, 179 (2004).
- [13] B. Farias, T. Passerat de Silans, M. Chevrollier, and M. Oria, *Phys. Rev. Lett.* **94**, 173902 (2005).
- [14] C. Masoller, T. Sorrentino, M. Chevrollier, and M. Oria, *IEEE J. Quantum Electron.* **43**, 261 (2007).
- [15] J. Javaloyes, J. Mulet, and S. Balle, *Phys. Rev. Lett.* **97**, 163902 (2006).
- [16] F. Rogister, D. Pieroux, M. Sciamanna, P. Megret, and M. Blondel, *Opt. Commun.* **207**, 295 (2002).
- [17] M. W. Lee, Y. H. Hong, and K. A. Shore, *IEEE Photonics Technol. Lett.* **16**, 2392 (2004).
- [18] R. Ju, P. S. Spencer, and K. A. Shore, *IEEE J. Quantum Electron.* **41**, 1461 (2005).
- [19] D. W. Sukow, A. Gavrielides, T. Erneux, M. J. Baracco, Z. A. Parmenter, and K. L. Blackburn, *Phys. Rev. A* **72**, 043818 (2006).
- [20] N. Shibasaki, A. Uchida, S. Yoshimori, and P. Davis, *IEEE J. Quantum Electron.* **42**, 342 (2006).
- [21] D. W. Sukow, A. Gavrielides, T. McLachlan, G. Burner, J. Amonette, and J. Miller, *Phys. Rev. A* **74**, 023812 (2006).
- [22] J. Houlihan, G. Huyet, and J. G. McInerney, *Opt. Commun.* **199**, 175 (2001).
- [23] D. L. Cheng, T. C. Yen, E. C. Liu, and K. L. Chuang, *IEEE Photonics Technol. Lett.* **16**, 1435 (2004).
- [24] G. Huyet, J. K. White, A. J. Kent, S. P. Hegarty, J. V. Moloney, and J. G. McInerney, *Phys. Rev. A* **60**, 1534 (1999).
- [25] C. Serrat, S. Prins, and R. Vilaseca, *Phys. Rev. A* **68**, 053804 (2003).
- [26] C. Serrat, B. Le Ny, and R. Vilaseca, *J. Opt. B: Quantum Semiclassical Opt.* **6**, 472 (2004).
- [27] J. K. White, J. V. Moloney, A. Gavrielides, V. Kovanis, A. Hohl, and R. Kalmus, *IEEE J. Quantum Electron.* **34**, 1469 (1998).
- [28] C. Serrat and C. Masoller, *Phys. Rev. A* **73**, 043812 (2006).
- [29] D. Pieroux, T. Erneux, and K. Otsuka, *Phys. Rev. A* **50**, 1822 (1994).
- [30] C. Masoller, M. S. Torre, and P. Mandel, *Phys. Rev. A* **71**, 013818 (2005).
- [31] P. R. Rice and H. J. Carmichael, *Phys. Rev. A* **50**, 4318 (1994).
- [32] F. Marin, A. Bramati, E. Giacobino, T. C. Zhang, J. Ph. Poizat, J. F. Roch, and P. Grangier, *Phys. Rev. Lett.* **75**, 4606 (1995).
- [33] J. Y. Law and G. P. Agrawal, *IEEE Photonics Technol. Lett.* **9**, 437 (1997).
- [34] J. Mulet, C. R. Mirasso, and M. San Miguel, *Phys. Rev. A* **64**, 023817 (2001).
- [35] A. M. Yacomotti, L. Furfaro, X. Hachair, F. Pedaci, M. Giudici, J. Tredicce, J. Javaloyes, S. Balle, E. A. Viktorov, and P. Mandel, *Phys. Rev. A* **69**, 053816 (2004).
- [36] M. Ahmed and M. Yamada, *IEEE J. Quantum Electron.* **38**, 682 (2002).
- [37] M. Ahmed, *Physica D* **176**, 212 (2003).
- [38] M. Yousefi, A. Barsella, D. Lenstra, G. Morthier, R. Baets, S. McMurtry, and J. P. Vilcot, *IEEE J. Quantum Electron.* **39**, 1229 (2003).